



Available online at [www.sciencedirect.com](http://www.sciencedirect.com)



C. R. Geoscience 339 (2007) 200–211

<http://france.elsevier.com/direct/CRAS2A/>

External geophysics, Climate and Environment (Glaciology)

## Palaeolatitude of glacial deposits and palaeogeography of Neoproterozoic ice ages

Ricardo I.F. Trindade <sup>a,\*</sup>, Mélina Macouin <sup>b</sup>

<sup>a</sup> Departamento de Geofísica, Instituto de Astronomia, Geofísica e Ciências Atmosféricas, Universidade de São Paulo, São Paulo, Brazil

<sup>b</sup> LMTG, UMR 5563, UR 154 CNRS, université Paul-Sabatier, IRD, OMP, 14, avenue Édouard-Belin, 31400 Toulouse, France

Received 7 December 2006; accepted after revision 19 February 2007

Available online 27 March 2007

Written on invitation of the Editorial Board

### Abstract

At the end of the Neoproterozoic, the Earth may have experienced important environmental changes, with a transition between two supercontinents (from Rodinia to Gondwana), extensive glaciations with ice caps reaching the Equator and the beginning of metazoan diversification. In such a context, the palaeomagnetic record can be used to constrain both the palaeogeography and the palaeoclimate (palaeolatitudinal distribution of glacial deposits). Here we present an up-to-date geochronological and palaeomagnetic database for the Neoproterozoic glacial deposits, including poles recently obtained on ‘cap carbonates’ from China, Oman, and Amazonia. The database comprises ten poles (from eight different cratons), obtained directly on the glacial deposits or on the overlying ‘cap carbonate’, and two other palaeolatitudes derived from reference poles coeval to well-dated glacial units in the same craton. The occurrence of glacial deposition at low latitudes ( $<30^\circ$ ) is attested by some good-quality poles, two of them well dated at  $\sim 740$  and  $\sim 635$  Ma. Based on these poles and on reference poles obtained on igneous rocks, tentative palaeogeographic reconstructions for  $\sim 750$ ,  $\sim 620$ , and  $\sim 580$  Ma (ages for which the database has limited but still sufficient entries) were performed in order to investigate the tectonic context within which the glacial events were produced. **To cite this article:** R.I.F. Trindade, M. Macouin, C. R. Geoscience 339 (2007).

© 2007 Published by Elsevier Masson SAS on behalf of Académie des sciences.

### Résumé

**Paléolatitude des dépôts glaciaires et paléogéographie des glaciations néoprotérozoïques.** À la fin du Néoprotérozoïque, la Terre a probablement été affectée par d'importants changements environnementaux, avec la transition entre deux supercontinents (du Rodinia au Gondwana), des glaciations sévères pendant lesquelles les calottes glaciaires atteignent la zone équatoriale, et le début de la diversification des métazoaires. Dans un tel contexte, les enregistrements paléomagnétiques peuvent être utilisés pour contraindre à la fois la paléogéographie et le paléoclimat (répartition paléolatitudinale des dépôts glaciaires). Nous présentons ici une base de données géochronologique et paléomagnétique pour les dépôts glaciaires néoprotérozoïques, incluant les pôles paléomagnétiques récemment acquis sur les *cap carbonates* de Chine, d'Oman et d'Amazonie. La base de données comporte dix pôles (de huit cratons différents), acquis directement sur les dépôts glaciaires ou sur les *cap carbonates* susjacentes, ainsi que deux autres paléolatitudes, qui proviennent de pôles de référence contemporains des unités glaciaires bien datées, du même craton. L'existence de dépôts glaciaires aux basses latitudes ( $<30^\circ$ ) est attestée par quelques pôles de bonne qualité, dont deux sont bien datés à 740 et 635 Ma. À partir de ces pôles, ainsi que des pôles de référence obtenus sur des roches ignées, des reconstitutions

\* Corresponding author.

E-mail address: [rtrindad@iag.usp.br](mailto:rtrindad@iag.usp.br) (R.I.F. Trindade).

paléogéographiques pour ~750, ~620 et ~580 Ma (âges pour lesquels la base de données comporte un nombre de résultats limité, mais encore suffisant) sont proposées, dans le but de préciser le contexte tectonique dans lequel se sont produits les événements glaciaires. **Pour citer cet article :** R.I.F. Trindade, M. Macouin, C. R. Geoscience 339 (2007).

© 2007 Published by Elsevier Masson SAS on behalf of Académie des sciences.

**Keywords:** Neoproterozoic; Palaeogeography; Palaeoclimate; Glaciation; Snowball Earth

**Mots clés :** Néoprotérozoïque ; Paléogéographie ; Paléoclimat ; Glaciation ; Terre boule de neige

## 1. Introduction

The Neoproterozoic is marked by severe changes in continental mass distribution, climate, and biological evolutionary trends (see [24] and references therein). In approximately 500 million years, continents have drifted from a Rodinia configuration, with most landmasses near the Equator by 1000 Ma, towards a Gondwana configuration at Cambrian times, assembling several continental blocks in the southern hemisphere (e.g., [37] and references therein). Between Rodinia dispersal and Gondwana assembly, the Earth's climate seems to have experienced strong oscillations. Glacial deposition occurred in most of the cratonic units during that time [22], some of them bearing low-inclination magnetizations, indicating that they were deposited near the Equator (e.g., [14,48]). These deposits are often covered by carbonate layers (cap carbonates) with negative carbon isotope signatures, which are interpreted as an effect of the rapid thaw of glaciers [26]. Whether the diamictite–carbonate successions were formed due to hard (*Snowball Earth*) or mild (*Slushball Earth*) global glacial events, or yet in Phanerozoic-like ice ages, is still a matter of debate.

The interest of palaeomagnetic data in constraining the Late Neoproterozoic environment is two-fold. On the one hand, it allows us to infer the latitude of deposition of the sedimentary deposits at a time when other proxies such as carbonates and evaporites may depart from their Phanerozoic distribution, and the fossil record does not provide palaeoclimatic information. On the other hand, it permits the reconstruction of the palaeogeography at the time of glacial episodes, which is of key importance to palaeoclimate models (e.g., [13,28]). In order to infer the palaeolatitude of sedimentary deposition, one needs either a direct palaeomagnetic result related to the sedimentary unit of interest or a good age constraint on the sedimentary deposits and a contemporaneous pole from the same continental block. Palaeomagnetic reconstruction, by its turn, demands good-quality poles from all the continents addressed in the reconstructions. Pole ages should match within a confidence limit so that plate

movements are negligible. Additional geological and isotopic information helps to overcome longitude and polarity ambiguities.

Two thorough reviews of the palaeomagnetic database for the Neoproterozoic glacial units were performed by Meert and Van der Voo [36] and Evans [15]. Interestingly enough, these compilations have depicted opposing scenarios, respectively contra and pro Neoproterozoic low-latitude glacial deposition (see commentaries in [15 (pp. 405–406)]). Since then, new palaeomagnetic poles were obtained on key cratonic units, such as Amazonia, southern and northwestern China, and Arabia, and some of the previous results were refined through new radiometric ages. In this contribution, we aim to provide the reader of this thematic issue with a concise and up-to-date review of the current palaeomagnetic evidence on the Neoproterozoic ice ages. We first present a selection of geochronological data in order to access the synchronicity of glacial events, and to delimit the time interval of our analysis. The ages on the glacial deposits will also be used to derive indirect palaeolatitude estimates based on coeval reference poles. Then, we present the latitudinal distribution of glacial deposits based on the most reliable palaeomagnetic data presently available for these units and the cap carbonates. Finally, these poles and other reference poles for the end of the Neoproterozoic are used to draw palaeogeographic scenarios into which the Neoproterozoic ice ages may have been produced.

## 2. Age of glacial events

The chronology of Neoproterozoic glacial deposits and the carbon isotope record of cap carbonates were recently reviewed by Halverson et al. [21]. Based on these data, these authors have proposed a triad of glacial events, named 'Sturtian', 'Marinoan', and 'Gaskiers'. In Table 1, we report the most reliable data listed by Halverson et al. [21], as well as new entries to this rapidly growing geochronological database. They comprise 25 U–Pb ages (ID-TIMS, SHRIMP and LA-ICPMS methods), most of them obtained from

Table 1

Reference geochronological data for Neoproterozoic glacial events

Tableau 1

Données géochronologiques de référence pour les événements glaciaires néoprotérozoïques

Age (Ma)	Method	Location	Unit (dated rock/mineral)	Significance	Reference
<b>Tasmania/Australia</b>					
575 ± 3	U-Pb SHRIMP	King Island	Grassy Gr. (zircon from intermediate sill)	<u>Minimum age of glacial deposition</u> (Cottons Breccia)	Calver et al. (2004) [6]
582 ± 4	U-Pb SHRIMP	Tasmania	Togari Gr. (zircon from riodacites within diamictites)	<u>Maximum age of glacial deposition</u> (Crolles Hill diamictite)	Calver et al. (2004) [6]
657 ± 17	U-Pb SHRIMP	Adelaide	Marino Arkose (detrital zircons)	<u>Maximum age of glacial deposition</u> (Marinoan)	Ireland et al. (1998) [29]
760 ± 12	U-Pb SHRIMP	Tasmania	Basement (zircons from granites)	<u>Maximum age of glacial deposition</u>	Turner et al. (1998) [55]
777 ± 7	U-Pb SHRIMP	Adelaide	Burra Gr. (zircons from volcanics)	<u>Maximum age of glacial deposition</u> (Julius River diamictite) <u>Maximum age of glacial deposition</u> (Sturtian)	Preiss (2000) [45]
<b>Southern China</b>					
<sup>a</sup> 621 ± 7	U-Pb SHRIMP	Yangtze Gorges	Doushantuo cap carbonate (zircon from tuff)	<u>Minimum age of glacial deposition</u> (2.3 m above Nantuo)	Zhang et al. (2005) [60]
<sup>a</sup> 635.2 ± 0.6	U-Pb TIMS	Yangtze Gorges	Doushantuo cap carbonate (zircon from tuff)	<u>Minimum age of glacial deposition</u> (2.3 m above Nantuo)	Condon et al. (2005) [9]
632.5 ± 0.5	U-Pb TIMS	Yangtze Gorges	Doushantuo cap carbonate (zircon from tuff)	<u>Minimum age of glacial deposition</u> (9.5 m above Nantuo)	Condon et al. (2005) [9]
663.3 ± 4.5	U-Pb TIMS	Eastern Guizhou	Datangpo Fm. (zircon from tuff)	<u>Maximum age of glacial deposition</u> (tuff ~150 m below Nantuo)	Zhou et al. (2004) [61]
<b>Northwestern China</b>					
727 ± 10	U-Pb SHRIMP	Tarim Block	Baiyisi Fm. (zircon from volcanics interbeded w/diamic.)	<b>Age of glacial deposition (Baiyisi)</b>	Huang et al. (2005) [27]
755 ± 15	U-Pb SHRIMP	Tarim Block	Baiyisi Fm. (zircon from volcanics, base of Baiyisi)	<u>Maximum age of glacial deposition (Baiyisi)</u>	Xu et al. (2005) [59]
<b>Baltica</b>					
620 ± 14	U-Pb LA-ICPMS	SE Norway	Rendalen Fm. (detrital zircon)	<u>Maximum age of glacial deposition (Moelv)</u>	Bingen et al. (2005) [2]
<b>Arabia</b>					
<sup>b</sup> 723 <sup>+16</sup> –10	U-Pb TIMS	Jebel Akhdar, Oman	Ghubrah Fm. (zircon from volcanics)	Age of glacial deposition (Ghubrah)	Brasier and Shield (2000) [4]
<sup>b</sup> 711.8 ± 1.6	U-Pb TIMS	Jebel Akhdar, Oman	<b>Ghubrah Fm. (zircon from volcanics)</b>	<b>Age of glacial deposition (Ghubrah)</b>	Allen et al. (2002) [1]
<b>Avalonia/Laurentia</b>					
580 ± 1	U-Pb TIMS	Newfoundland	<b>Gaskiers Fm. (zircon from tuff)</b>	<b>Age of glacial deposition (Gaskiers)</b>	Bowring et al. (2003) [3]
595 ± 2	U-Pb TIMS	Boston Basin	Squantum tillite (zircon from tuff's fragment)	Maximum age of glacial deposition (Squantum tillite)	Thompson & Bowring (2000) [51]
601 ± 4	U-Pb TIMS	Dalradian, Scotland	Tayvallich Fm. (zircon from tuff)	<u>Minimum age of glacial deposition</u> (Port Askaig)	Dempster et al. (2002) [12]
685 ± 1	U-Pb SHRIMP	Idaho	<b>Edwardsburg Fm. (zircon from volcanics)</b>	<b>Age of glacial deposition (Edwardsburg)</b>	Lund et al. (2003) [34]

Table 1 (Continued)  
Tableau 1 (Suite)

Age (Ma)	Method	Location	Unit (dated rock/mineral)	Significance	Reference
<b>709 ± 5</b>	<b>U–Pb SHRIMP</b>	<b>Idaho</b>	<b>Pocatello Fm. (zircon from tuff, base of Pocatello)</b>	<b>Age of glacial deposition (Scout Mountain)</b>	<b>Fanning &amp; Link (2004) [18]</b>
755 ± 18	U–Pb TIMS	NW Canada	Granite pebble in Rapitan Gr. diamictite	Maximum age of glacial deposition (Rapitan)	Ross & Villeneuve (1997) [46]
<b>Kalahari</b>	<b>Pb–Pb evap.</b>	<b>South Namibia</b>	Rosh Pinah Fm. (zircon from acid volcanic)	<b>Minimum age of glacial deposition (Kaigas)</b>	Frimmel et al. (1996) [20]
<i>Congo/São Francisco</i>					
<b>635.5 ± 1.2</b>	<b>U–Pb TIMS</b>	<b>North Namibia</b>	<b>Ghaub Fm. (zircon from volcanic ash)</b>	<b>Age of glacial deposition (Ghaub)</b>	<b>Hoffman et al. (2004) [23]</b>
746 ± 2	U–Pb TIMS	North Namibia	Naauwpoort Fm. (zircon from acid volcanics)	Maximum age of glacial deposition (Chuos)	Hoffman et al. (1996) [25]
<b>735 ± 5</b>	<b>U–Pb SHRIMP</b>	<b>Zambia</b>	<b>Kundelungu Gr. (zircon from mafic volcanics)</b>	<b>Age of glacial deposition (Grand Conglomerat)</b>	<b>Key et al. (2001) [30]</b>

Note: Ages in bold were obtained directly on the glacial units, and constitute the direct constraints available for the Neoproterozoic ice ages. Other ages are either maximum or minimum ages.  
 a indicates ages obtained in different studies performed on equivalent samples (collected at the same stratigraphic level and same location).  
 b indicates ages obtained in different studies performed on equivalent samples (collected at the same stratigraphic level and same location).

zircon crystals extracted from tuffs, ash beds or volcanic rocks, or yet from detrital grains separated from the glacial rocks. Eight results give direct constraints on the age of glacial sedimentation for the following units: *Baiyisi (or Beiyixi)* (Tarim) [27], *Ghubrah* (Arabia) [1,4], *Gaskiers* (Avalonia) [39], *Edwardsburg* (western Laurentia) [34], *Scout Mountain* (western Laurentia) [18], *Ghaub* (Kaoko belt) [23] and the *Grand Conglomérat* (eastern Congo craton) [30]. Data from tuffs 2.3 m and 9.5 m above the *Nantuo* glacial deposits constrain the end of glacial deposition in southern China [9,61]. Other results correspond to maximum ages (e.g., detrital zircons) or minimum ages (e.g., ages of intrusive rocks) for the deposition of glacial units.

Age distribution is shown in Fig. 1. The older glacial units, usually embodied into the ‘Sturtian’ glaciation, present the largest number of ages. They show a large spread between 750 and 670 Ma, including a set of glacial successions with ages around 750 Ma (Kaigas, Grand Conglomerat), the Baiyisi glacials with ages between 755 and 727 Ma (volcanics interbedded with diamictites), and younger units with ages ranging from 710 to 670 Ma (Ghubrah, Edwardsburg, Pocatelo). Either they represent different discrete glacial events, or the Sturtian glaciation is a protracted event encompassing almost 80 Ma. The younger events have a more limited number of ages. In spite of that, it is worth noting the coincident end of glacial events in Namibia and China constrained by high-precision ID-TIMS dating [9,23]. These data, obtained on different cratons, point to an age of around 635 Ma for the ‘Marinoan’ event. However, the actual age of the Marinoan glacial deposits in Australia is poorly defined. A maximum age of  $657 \pm 17$  Ma is given by detrital zircons in the underlying Marino Arkose [29], but much younger ages have been suggested based on purportedly correlative deposits recently dated at  $\sim 580$  Ma in Tasmania [6]. Ages within  $580 \pm 1$  Ma were also obtained for tuffs collected below, within and above the Gaskiers Formation (not fully published yet: see abstract by [3]). The Squantum tillite (Boston basin), the Loch na Cille Boulder Bed (Dalradian) and the Moelv tillite (Norway) are usually correlated with the Gaskiers Formation. The age of the Squantum tillite is bracketed between 595 and 570 Ma [51]. Maximum ages of 601 and 620 Ma were obtained, respectively, for Loch na Cille and the Moelv tillite [2,12]. Although these data do not rule out correlation, the deposits of Gaskiers, Squantum, Loch na Cille and Moelv could equally represent distinct, short-lived glacial incursions.

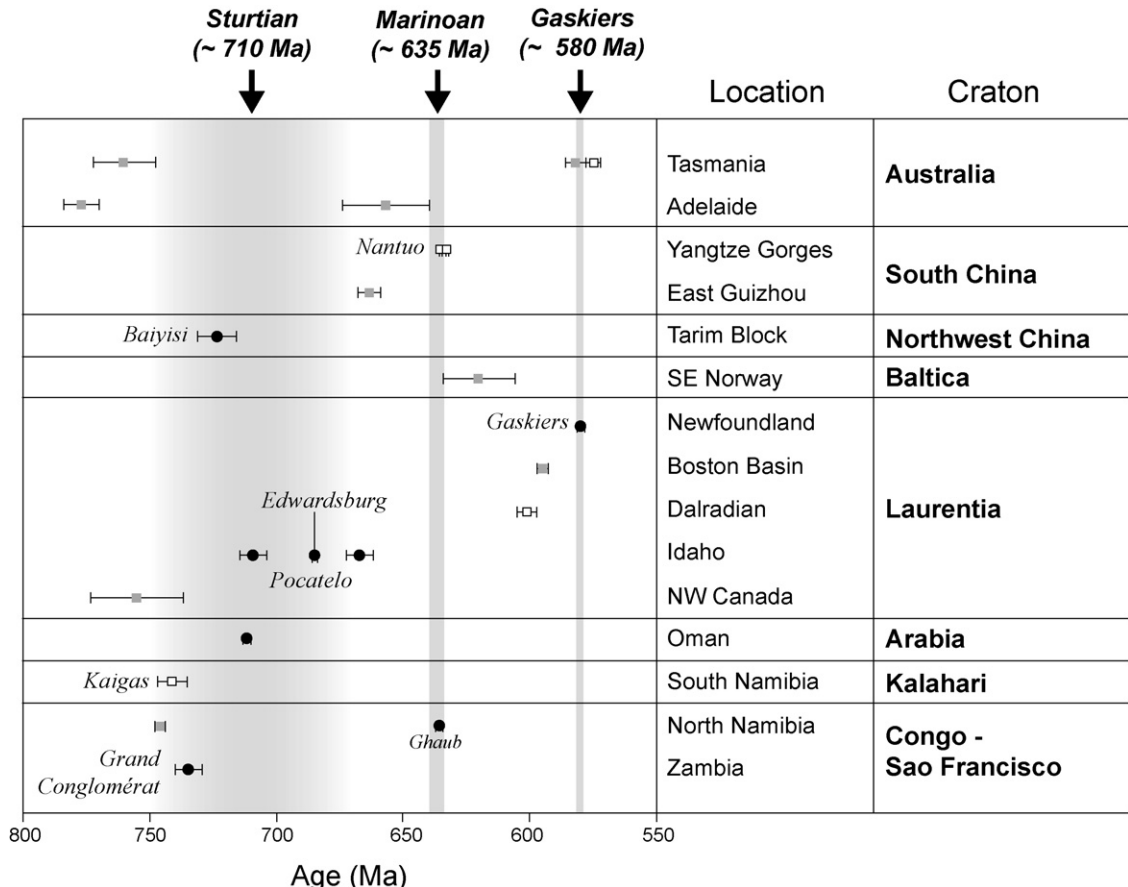


Fig. 1. Age of Neoproterozoic glacial deposits. Filled black circles are data obtained directly on the (quoted) glacial unit. Empty and full (grey) squares are minimum and maximum age constraints. Grey, vertical bars indicate the three glacial intervals usually referred to in the literature.

Fig. 1. Âge des dépôts glaciaires néoprotérozoïques. Les cercles noirs pleins correspondent aux données obtenues directement sur l'unité glaciaire (citéée). Les carrés (gris) vides et pleins représentent les contraintes d'âge minimum et maximum. Les barres verticales grises indiquent les trois intervalles glaciaires couramment répertoriés dans la littérature.

### 3. Palaeolatitude of glacial deposits

In Table 2, we list ten poles obtained directly from the glacial units, or alternatively from the cap carbonates, for which the magnetization is considered to be primary in origin. In selecting these poles, we have picked only those for which stability tests ascertain the primary (depositional or early-diagenetic) nature of the magnetization. They are: *Elatina Formation* (Central Australia) [47,48], *Walsh cap carbonate* (NW Australia) [33], *Doushantuo Formation* (South China) [35], *Nyborg Formation* (Baltica) [52], *Huqf Supergroup* (Arabia) [31], *Rapitan Group* (western Laurentia) [42], *Squantum Member* (Avalonia) [17], *Puga cap carbonates* (Amazonia) [54], and *La Tinta Formation* (Rio de la Plata) [56]. The pole for *Baiyisi* (Tarim) [27], obtained on volcanic rocks interbedded within the

glacial deposits of that unit, is regionally consistent after tilt correction, and was thus included into the list, despite the lack of a robust stability test. Good age constraints are available for three of these poles: *Baiyisi*, *Doushantuo*, and *Squantum*.

In addition to the ten poles listed above, palaeolatitudinal information could also be gathered from reference poles contemporaneous to the remaining well-dated glacial deposits from Arabia, Laurentia, and Congo–São Francisco. Unfortunately, there is no strict coincidence in age between available reference poles and these glacial deposits, but palaeolatitudes can be tentatively attributed to the *Grand Conglomerat* ( $735 \pm 5$  Ma) and the base of *Pocatello* ( $709 \pm 5$  Ma), based on the *Mbozi complex* ( $755 \pm 25$  Ma) [39] and the *Franklin dykes* ( $723 \pm 25$  Ma) [5,7] poles, respectively. Laurentia lacks reference poles between 720 and

Table 2  
Palaeomagnetic poles for glacial units or cap carbonates, and reference poles for the Neoproterozoic

Tableau 2  
Pôles paléomagnétiques pour les unités glaciaires et les *cap carbonates* et pôles de référence pour le Néoprotérozoïque

	Craton/Unit	Age(Ma)	Direction		Palaeomagnetic pole		Precision			A95	Plat	Quality index							Reference		
			Dec	Inc	Lat	Lon	N	n	dp			1	2	3	4	5	6	7	Q		
Tasmania/Australia		Max																			
1	Elatina Fm. (1)	657 (max)	197	-5	-52	347	10	79	3.7	7.4	5.7	7.4	2.5 ± 3.7	0	0	1	1	1	0	4	Schmidt & Williams (1995) [47]
1	Elatina Fm. (2)	657 (max)	212	-17	-40	2	58	126	3.3	6.4	9.9	6.2	8.7 ± 3.1	0	1	1	1	1	1	6	Sohl et al. (1999) [48]
	<i>Yaltipena Fm.</i>	657 (max)	204	-16	-44	353	16	36	5.9	11.4	12.2	11.0	8.2 ± 5.5	0	1	1	1	1	0	5	Sohl et al. (1999) [48]
2	Walsh tillite ‘cap dolostone’	?	149	-63	-21	282	5	27	12.2	15.4	62.3	9.8	44.5 ± 4.9	0	0	1	1	1	1	5	Li (2000) [33]
	Mundine Well dikes	755 ± 3	15	31	45	135	14	116	4.1	4.1	—	5.0	16.7 ± 2.5	1	0	1	1	1	0	5	Wingate & Giddings (2000) [58]
Southern China		Max																			
3	Doushantuo Fm.	632.5 ± 0.5	271	-7	1	197	7	80	4.5	9.0	45.0	9.1	3.5 ± 4.6	1	0	1	1	1	1	6	Macouin et al. (2003) [35]
	<i>Liantuo Fm.</i> (pole CIT)	748 ± 12	288	-53	3	164	—	106	2.1	2.7	59.0	1.8	33.6 ± 0.9	1	1	1	0	1	1	6	Evans et al. (2000) [15]
	<i>Liantuo Fm.</i> (pole UWA)	748 ± 13	276	-57	14	165	—	13	7.0	9.6	40.0	6.6	37.6 ± 3.3	1	0	1	0	1	0	4	Evans et al. (2000) [15]
Northwestern China		Max																			
4	Baiyisi volcanics	727 ± 10	245	2	-18	14.2	6	43	3.0	6.0	124.7	6.0	1.0 ± 3.0	1	0	1	0	1	0	4	Huang et al. (2005) [27]
Baltica		Max																			
5	Nyborg Fm.	620 (max)	110	52	24.3	88.5	6	55	17.1	24.9	14.6	18.0	32.6 ± 9.0	0	0	1	1	1	0	3	Torsvik et al. (1995) [52]
	Egersund dolerites	616 ± 3	119	61	22	50	4	35	16.4	21.4	44.0	14.0	42.1 ± 7.0	1	1	1	0	1	0	4	Poorter (1972) [44]
Arabia		Max																			
6	Huqf Supergorup	?	169	28	-52	74	25	86	4.4	8	16.7	7.3	14.9 ± 3.7	0	1	1	1	1	1	6	Kilner et al. (2005) [31]
	<i>Dokhan Volcanic Fm.</i>	593 ± 15	178	37	-43	36	10	49	7.0	11.0	33.0	10.0	20.6 ± 5.0	1	1	1	0	1	0	4	Davies et al. (1980) [11]
Avalonia/Laurentia		Max																			
7	Rapitan Gr.	755 (max)	261	12	-1	334	10	25	4.0	9.0	34.0	8.0	6.1 ± 4.0	0	0	1	1	1	0	4	Park (1997) [42]
8	Squantum Mb.	595 (max)	219	71	13	267	4	13	7.9	9.0	311.2	5.2	55.4 ± 2.6	0	0	1	1	0	1	3	Fang et al. (1986) [17]
	<i>Catoctin A</i>	564 ± 8	68	84	-42	117	6	28	17.4	17.7	59.0	9.0	78.1 ± 3.0	1	1	0	0	1	1	5	Meert et al. (1994) [38]
	<i>Catoctin B</i>	564 ± 9	92	17	-4	184	9	50	6.9	13.4	16.0	13.0	8.7 ± 7.0	1	1	1	0	0	1	4	Meert et al. (1994) [38]
	<i>Sept-Îles Complex B</i>	565 ± 3	105	82	-44	135	16	76	9.7	9.9	53.2	5.1	74.3 ± 9.6	1	1	1	0	1	1	5	Tanczyk et al. (1987) [50]
	<i>Sept-Îles Complex A</i>	565 ± 4	333	-29	20	141	10	51	5.0	9.0	34.0	8.0	15.5 ± 4.9	1	1	1	1	1	0	5	Tanczyk et al. (1987) [50]
	<i>Callander Complex</i>	575 ± 5	82	83	-46	121	26	205	5.9	6.1	83.0	3.1	76.2 ± 5.9	1	1	1	1	1	1	6	Symons & Chiasson (1990) [49]
	<i>Long Range dykes</i>	614 ± 6/-4	125	56	12	346	12	69	18.3	25.7	48.0	18.0	36.5 ± 19.4	1	0	1	0	1	1	4	Murthy et al. (1992) [41]
	<i>Franklin dykes</i>	723 ± 4/-2	124	1	9	153	13	82	2.6	5.3	63.0	5.0	0.5 ± 2.5	1	1	1	1	1	0	6	Christie & Fahrig (1983) [7]
																				See also Buchan et al. (2000) [5]	
Congo/Sao Francisco		Max																			
	<i>Mbozi Complex</i>	755 ± 25	320	16	46	325	10	64	5	9	32	9	8.2 ± 4.8	0	1	1	0	1	1	5	Meert et al. (1995) [39]
West Africa		Max																			
	<i>Adma Diorite</i>	616 ± 11	317	79	34	344	13	62	16.1	17.1	22.0	9.0	68.8 ± 16.0	1	1	1	0	0	0	3	Morel (1981) [40]
Amazonia		Max																			
9	<i>Puga cap carbonates A</i>	623 ± 15?	181	39	51	249	13	51	6.0	9.0	—	8.0	22.0 ± 5.7	0	1	1	1	1	1	5	Trindade et al. (2003) [54]

Table 2 (Continued)  
Tableau 2 (Suite)

	Craton/Unit	Age(Ma)	Direction	Palaeomagnetic pole	Precision	A95	Plat	Quality index						
		Dec	Inc	Lat	n	dp	dm	1 2 3 4 5 6 7 Q Reference						
Rio de la Plata/Luis Alves 10	La Tinta Fm. <i>Campo Alegre Gp.</i>	? 598 ± 29	360 36	−66 −40	79 57	121 43	5 6	4.8 46	4.8 9.0	17.0 56.0	5.0 10.0	48.3 ± 6.7 22.8 ± 7.3	0 1 0 1 1 1 1 5 1 1 1 0 1 1 6	Valencio et al. (1980) [56] D’Agrella-Filho & Paccia (1988) [10]
India	<i>Malani Igneous suite</i>	760 ± 12	9	65	68	88	9	85	12.7	15.7	29.4	9.7	47.0 ± 12.7	1 1 1 0 1 6 Torsvik et al. (2001) [53]

Note: Numbered poles (1 to 11) are from glacial deposits or cap carbonates. Other entries (in italics) are reference poles used to indirectly constrain the glacial events in each craton. N = number of sites; n = number of demagnetized samples used to calculate the palaeomagnetic pole. Q-index criteria (1–7) (Van der Voo [57]) are summarized as follows: (1) good age constraints for the magnetization, (2) statistical precision ( $A95 < 16$ ) from adequate sample number ( $>24$ ), (3) detailed demagnetization with vector subtraction, and principal-component analysis, (4) field tests constraining the timing of magnetization, (5) structural control/continuity with the craton, (6) presence of reversals, and (7) dissimilarity from more recent palaeomagnetic direction.

620, thus hindering any palaeolatitudinal control on the Edwardsburg Formation, and the end of Pocatello deposition ( $\sim 670$  Ma). There are also no poles for Arabia at the time of the Ghubrah glacial deposition ( $711.8 \pm 1.6$  Ma).

Palaeolatitudes vary from near the palaeo-Equator to moderate and high latitudes (Fig. 2). It is worth noting that even after the inclusion of recent poles and applying restrictive screening to the database, we still observe the low-latitude cluster previously recognized by Chumakov and Elston [8] and Evans [15]. Indeed, several high-rank palaeomagnetic data (Q-index 5 or higher: see Table 2) give low latitudes for the glacial deposition (Fig. 2a). These results include, not only palaeomagnetic poles obtained on sedimentary units, for which post-depositional inclination–shallowing could introduce a low-latitude bias, but also poles obtained in interbedded volcanics (Baiyisi). Estimates transferred from reference poles to well-dated glacial deposits also give palaeolatitudes below  $15^\circ$  (Fig. 2b). Palaeolatitudes higher than  $30^\circ$  are recorded in four units, even reaching  $55^\circ$  for the Squantum tillite. The large age uncertainty for most palaeomagnetic entries (denoted by the long empty rectangles in Fig. 2b) frustrates any attempt to recover the latitudinal distribution of glacial deposits through time. Nevertheless, results from Baiyisi ( $\lambda = 1 \pm 3^\circ$ ) and Doushantuo ( $\lambda = 3.5 \pm 4.6^\circ$ ) indicate that ice caps did reach the Equator  $\sim 740$  and  $\sim 635$  Ma ago.

#### 4. Palaeogeographic reconstructions

The Neoproterozoic glacial episodes occurred between the demise of the supercontinent Rodinia and the assembly of Gondwana. Several Rodinia configurations were proposed in the last decade, implying different connections of cratonic units with Laurentia, which is the central piece in all reconstructions (see review in [37]). In Fig. 3, we propose four palaeogeographic configurations for three periods:  $\sim 750$ , 620, and 580 Ma, respectively. We note, however, that these reconstructions are based on a rather limited number of poles (only cratons in dark colour have latitudinal constraints), most of them with slightly different ages within 30 Ma. Thus, these Neoproterozoic palaeomaps should be taken as very sketchy.

The first interval of widespread glacial deposition occurs at around 750 Ma, some millions of years after the break-up of Rodinia along the western margin of Laurentia [58]. The corresponding reconstruction (Fig. 3a) is based on reference poles from Australia

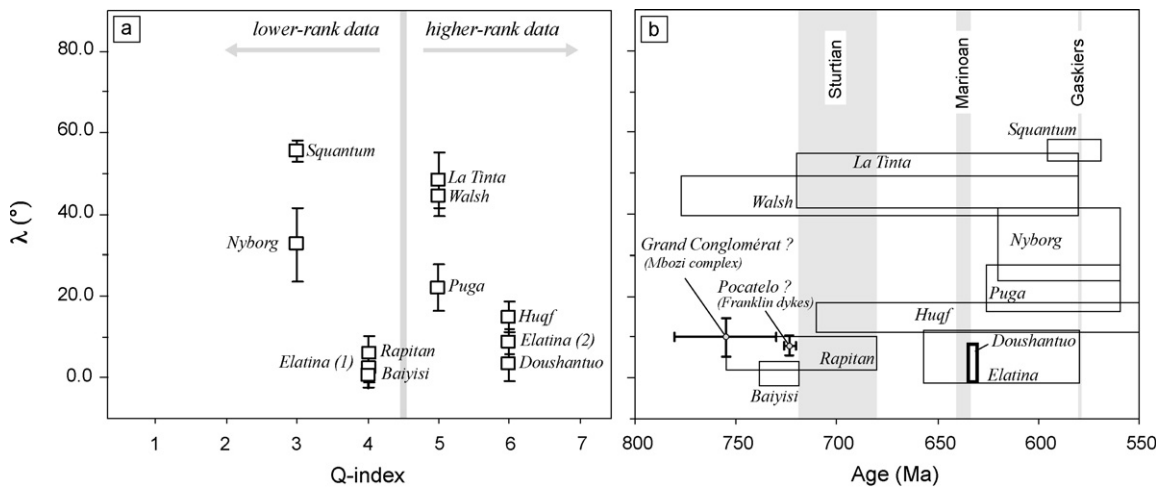


Fig. 2. Palaeolatitude estimates on the Neoproterozoic glacial deposits and cap carbonates. (a) Palaeolatitude ( $\lambda$ ) with error bars against Q-index [57]. (b) Palaeolatitude against age. Height and length of rectangles indicate error estimates in palaeolatitude and age, respectively. Palaeolatitude estimates obtained from reference poles (Mbozi complex and Franklin dykes) are shown in (b), with error bars for latitude and age.

Fig. 2. Estimations de paléolatitudes obtenues pour les dépôts glaciaires et les *cap carbonates* néoprotérozoïques. (a) Paléolatitude ( $\lambda$ ) avec barres d'erreur, en fonction de l'index-Q [57]. (b) Paléolatitude en fonction de l'âge. La hauteur et la longueur des rectangles indiquent, respectivement, les estimations d'erreur en paléolatitude et en âge. Les estimations de paléolatitudes obtenues à partir des pôles de référence (complexe de Mbozi et dykes de Franklin) sont indiquées en (b), avec les barres d'erreur pour la latitude et l'âge.

(Mundine Well dykes;  $755 \pm 3$  Ma), southern China (Liantuo Formation;  $748 \pm 12$  Ma) [16], northwestern China (Baiyisi volcanics; 755–727 Ma) [27], Congo–São Francisco (Mbozi Complex;  $755 \pm 25$  Ma) [39] and India (Malani Igneous suite;  $760 \pm 12$  Ma) [53]. Laurentia was positioned according to the slightly younger Franklin dykes pole ( $723^{+4/-}$  Ma) [5,7]. Australia, Antarctica, and South China are represented separated from Laurentia as a consequence of the proto-Pacific rift. The Tarim block, northwestern China, is placed close to southern China and Australia, following Huang et al. [27]. The Congo–São Francisco craton and the adjoining cratonic fragments (East-Sahara, Luis Alves, and Parana) are also represented separated from the other cratons. A large oceanic domain is inferred along the (present-day) western margin of the Congo–São Francisco block based on protracted collisional events from 940 up to 630 Ma [43].

The next interval of interest corresponds to the ‘Marinoan’ event marked by the coincident dates of 635 Ma for Doushantuo (Nantuo cap carbonate) and Ghaub Formations. For this time, the Doushantuo pole [35] suggests a low-latitude deposition of the underlying Nantuo glacial deposit. However, no other poles are available for the same age. Thus, a reconstruction for  $\sim 620$  is presented in Fig. 3b, which may represent approximately the palaeogeography by the time of the Nantuo/Ghaub (‘Marinoan’) event. In such a reconstruction, Laurentia is positioned at low latitudes

according to the long-range dykes pole ( $614^{+6/-}$  Ma) [41], Baltica is placed according to the Egersund dolerites ( $616 \pm 3$  Ma) [44], and West Africa is placed according to the Adma diorite ( $616 \pm 11$  Ma) [40]. The approximate position of southern China is based on the Doushantuo pole ( $632.5 \pm 0.5$  Ma) [35]. In addition, we have used the poles of Puga and Huqf to position Amazonia and Arabia, assuming that their ages are closer to the ‘Marinoan’ event, as suggested by Trindade et al. [54] and Kilner et al. [31], respectively. The position of the Congo–São Francisco is tentatively placed on this reconstruction using the Dokhan volcanics pole [12]. This pole was obtained from Egypt, which has already joined the eastern Saharan craton at this time and, in spite of its younger age of  $593 \pm 15$  Ma, it is the best available constraint to the position of central Gondwanan blocks. The position of other cratonic units is still more uncertain, due to the lack of reliable contemporaneous poles. Fig. 3a and b, although still poorly constrained, suggest that, by  $\sim 620$  Ma, most landmasses have preferentially occupied low latitudes. Interestingly enough, this palaeogeography has strong implications on global climate.

The last interval of interest at around 580 Ma comprehends the short-lived Gaskiers glaciation and its possible correlatives, Squantum, Loch na Cille, and Moelv. However, palaeogeographic models between 590 and 560 Ma are highly controversial, due to the

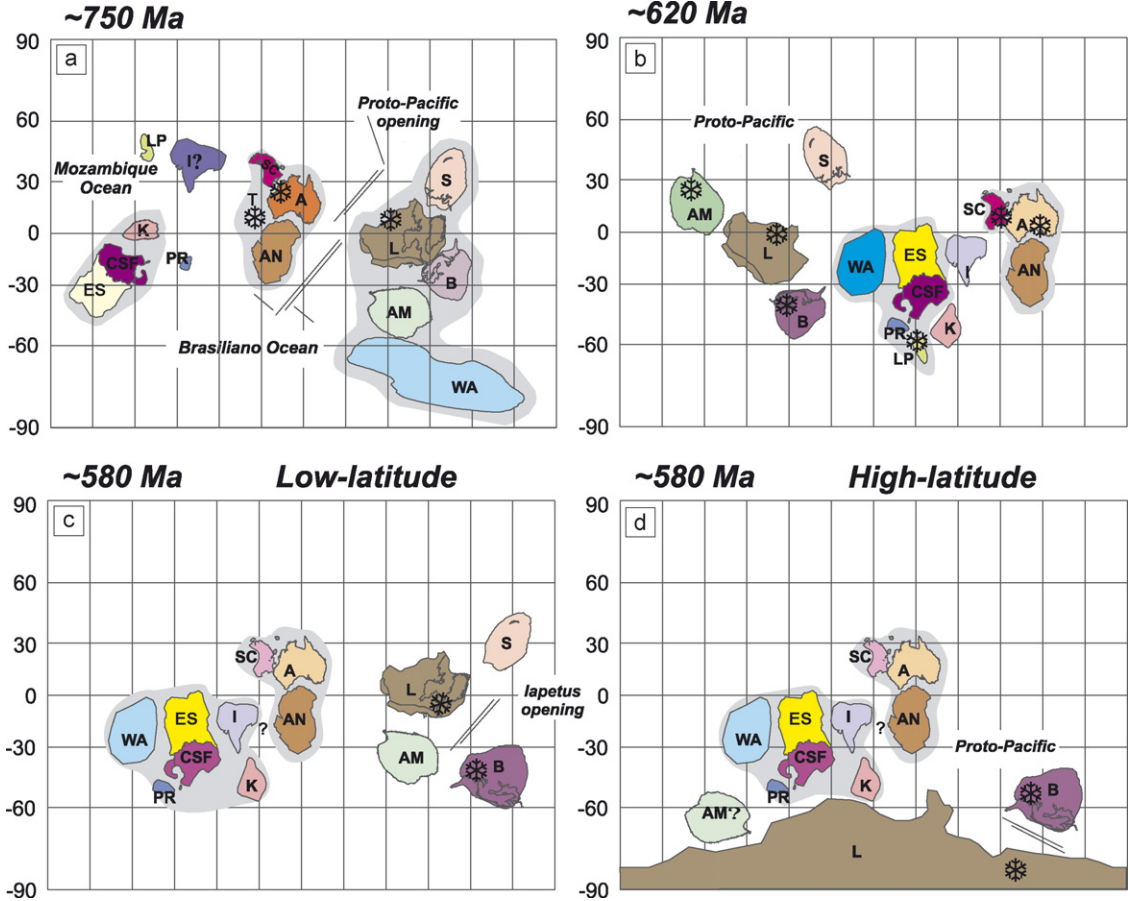


Fig. 3. Palaeogeographic reconstructions between 750 and 580 Ma based on the palaeopoles given in Table 2. Shaded areas around some groups of blocks delineate the large palaeogeographic blocks. The position of glacial units is depicted by snowflakes. See text for details. I = India; M = Madagascar; AN = Antarctica; A = Australia; S = Siberia; L = Laurentia; B = Baltica; ES = East-Sahara block; T = Tarim block, CGM = Coats Land/Grunehogna/Maudheim; K = Kalahari; CSF = Congo-São Francisco; LP = Rio de la Plata; AM = Amazonia; RA = Rio Apa; PR = Paraná; WA = West Africa.

Fig. 3. Reconstitutions paléogéographiques entre 750 et 580 Ma basées sur les paléopôles présentés dans le Tableau 2. Les zones ombrées autour de certains groupes de blocs délimitent de larges blocs paléogéographiques. La position des unités glaciaires est indiquée par des flocons de neige. Voir le texte pour les détails.

ambiguous results presented by the Laurentian poles. Two studies [38,50] of well-dated igneous complexes (Catoctin and Sept-Îles) have isolated a pair of magnetic components, giving either high latitudes or low latitudes for Laurentia at  $\sim 580$  Ma (see Table 2). Here we show two alternative palaeogeographic models that account for low latitudes (Fig. 3c) and high latitudes (Fig. 3d). In the low-latitude model, we have used the Catoctin B ( $564 \pm 8$  Ma) and Sept-Îles A ( $565 \pm 3$  Ma) for Laurentia. In the high-latitude model, Laurentia was positioned according to the following poles: Callander Complex pole ( $575 \pm 5$  Ma) [49], Catoctin A ( $564 \pm 8$  Ma), and Sept-Îles B ( $565 \pm 3$  Ma). If the latter configuration is confirmed, then a rapid shift in distribution of landmasses has occurred between 620

and 580 Ma. The glacial units observed in eastern Laurentia, Baltica, Cadomia, and Avalonia occupy high latitudes, and could thus have been produced in Phanerozoic-like conditions.

The position of continental landmasses has a strong influence on the climate [19]. Several authors have claimed that the equatorward distribution of continents at the Neoproterozoic might have induced strong weathering, leading to the drawdown of CO<sub>2</sub> necessary to trigger the glacial events (e.g., [24,32]). However, whether landmasses are grouped (supercontinents) or dispersed also plays a role in regulating the sink of CO<sub>2</sub> through weathering. Applying a coupled climate-geochemical model, Donnadieu et al. [13] have shown that the dispersal of Rodinia engenders the enhancing of

$\text{CO}_2$  consumption, due to the larger runoff on the total length of continental margins. This mechanism could pave the way for events of severe (even global) glaciation. If low-latitude palaeogeographies with dispersed continental masses have prevailed between the demise of Rodinia and the final assembly of Gondwana (Fig. 3a–c), such mechanism could explain the dominantly cold climate of that time, sometimes falling into deep freeze (equatorial ice caps).

## 5. Conclusions

Geochronological and palaeomagnetic data for the Neoproterozoic glacial deposits and cap carbonates attest the widespread occurrence of glacial deposition at low latitudes ( $<30^\circ$ ) between 750 and 570 Ma. Well-dated poles constrain at least two advances of ice caps down to the Equator at 730 and 635 Ma. Palaeogeographic reconstructions based on reference poles suggest a dominantly equatorial position of several cratons throughout the Cryogenian with possible consequences on the dominantly ice-house climate of that time.

## Acknowledgments

We warmly thank A. Nédélec for her thorough review and the editorial handling of this manuscript. L.C. Vieira has given invaluable help with final edition of figures and text. This work is financed by FAPESP (05/53231-1) through the Eclipse program (CNRS).

## References

- [1] P. Allen, S.A. Bowring, J. Leather, M. Brasier, A. Cozzi, J. Grotzinger, G. McCarron, J. Amthor, Chronology of Neoproterozoic glacials: new insights from Oman, in: 16th International Sedimentological Congress, Johannesburg, Abstracts, 2002, pp. 7–8.
- [2] B. Bingen, W. Griffin, T. Torsvik, A. Saeed, Timing of Late Neoproterozoic glaciations on Baltica constrained by detrital geochronology in the Hedmark Group, Southeast Norway, *Terra Nova* 17 (2005) 250–258.
- [3] S. Bowring, P. Myrow, E. Landing, J. Ramezani, J. Grotzinger, Geochronological constraints on terminal Proterozoic events and the rise of metazoans, *Geophys. Res. Abstr. (EGS, Nice)* 5 (2003) 13219.
- [4] M.D. Brasier, G. Shields, Neoproterozoic chemostratigraphy and correlation of the Port Askaig glaciation, Dalradian of Scotland, *J. Geol. Soc. Lond.* 157 (2000) 909–914.
- [5] K.L. Buchan, S. Mertanen, R.G. Park, L.J. Pesonen, S.-A. Elming, N. Abrahamsen, G. Bylund, Comparing the drift of Laurentia and Baltica in the Proterozoic: the importance of key palaeomagnetic poles, *Tectonophysics* 319 (2000) 167–198.
- [6] C.R. Calver, L.P. Black, J.L. Everard, D.B. Seymour, U–Pb zircon age constraints on Late Neoproterozoic glaciation in Tasmania, *Geology* 32 (2004) 893–896.
- [7] K.W. Christie, W.F. Fahrig, Paleomagnetism of the Borden dykes of Baffin Island and its bearing on the Grenville Loop, *Can. J. Earth Sci.* 20 (1983) 275–289.
- [8] N.M. Chumakov, D.P. Elston, The paradox of Late Proterozoic glaciations at low latitudes, *Episodes* 12 (1989) 115–120.
- [9] D. Condon, M. Zhu, S.A. Bowring, A. Yang, Y. Jin, U–Pb Ages from the Neoproterozoic Doushantuo Formation, China, *Science* 308 (2005) 95–98. , doi:10.1126/science.1107765.
- [10] M.S. D’Agrella-Filho, I.G. Pacca, Paleomagnetism of the Itajaí, Castro and Bom Jardim Groups from southern Brazil, *Geophys. J.* 93 (1988) 365–376.
- [11] J. Davies, A.E.M. Nairn, R. Ressetar, The paleomagnetism of certain Late Precambrian and Early Paleozoic rocks from the Red Sea Hills, Eastern Desert, Egypt, *J. Geophys. Res.* 85 B7 (1980) 3699–3710.
- [12] T.J. Dempster, G. Rogers, P.W.G. Tanner, B.J. Bluck, R.J. Muir, S.D. Redwood, T.R. Ireland, B.A. Paterson, Timing of deposition, orogenesis and glaciation within the Dalradian rocks of Scotland: Constraints from U–Pb zircon ages, *J. Geol. Soc. Lond.* 159 (2002) 83–94.
- [13] Y. Donnadieu, Y. Goddard, G. Ramstein, A. Nédélec, J. Meert, A ‘snowball Earth’ climate triggered by continental break-up through changes in run-off, *Nature* 428 (2004) 303–306.
- [14] B.J.J. Embleton, G.E. Williams, Low palaeolatitude of deposition for Late Precambrian periglacial varvites in South Australia: implications for palaeoclimatology, *Earth Planet. Sci. Lett.* 79 (1986) 419–430.
- [15] D.A.D. Evans, Stratigraphic, geochronological, and paleomagnetic constraints upon the Neoproterozoic climatic paradox, *Am. J. Sci.* 300 (2000) 347–443.
- [16] D.A.D. Evans, Z.X. Li, J.L. Kirschvink, M.T.D. Wingate, A high-quality Mid-Neoproterozoic paleomagnetic pole from South China, with implications for ice ages and the breakup configuration of Rodinia, *Precambrian Res.* 100 (2000) 313–334.
- [17] W. Fang, R. Van der Voo, R.J.E. Jonson, Eocambrian paleomagnetism of the Boston basin: Evidence for a displaced terrane, *Geophys. Res. Lett.* 13 (1986) 1450–1453.
- [18] C.M. Fanning, P.K. Link, U–Pb SHRIMP ages of Neoproterozoic (Sturtian) glaciogenic Pocatello Formation, southeastern Idaho, *Geology* 32 (2004) 881–884.
- [19] F. Fluteau, G. Ramstein, J. Besse, Simulating the evolution of the Asian and Africa monsoons during the past 30 millions years using an atmospheric general circulation model, *J. Geophys. Res.* 104 (1999) 11995–12018.
- [20] H.W. Frimmel, U.S. Klötzli, P.R. Siegfried, New Pb–Pb single zircon age constraints on the timing of Neoproterozoic glaciation and continental break-up in Namibia, *J. Geol.* 104 (1996) 459–469.
- [21] G.P. Halverson, P.F. Hoffman, D.P. Schrag, A.C. Maloof, A.H. Rice, Toward a Neoproterozoic composite carbon-isotope record, *Geol. Soc. Am. Bull.* 117 (9/10) (2005) 1181–1207.
- [22] W.B. Harland, Critical evidence for a great infra-Cambrian glaciation, *Geol. Rundsch.* 54 (1964) 45–61.
- [23] K.H. Hoffmann, D.J. Condon, S.A. Bowring, J.L. Crowley, U–Pb zircon date from the Neoproterozoic Ghaub Formation, Namibia: Constraints on Marinoan glaciation, *Geology* 32 (2004) 817–820. , doi:10.1130/G20519.1.
- [24] P.F. Hoffman, D.P. Schrag, The snowball Earth hypothesis: Testing the limits of global change, *Terra Nova* 14 (2002) 129–155.

- [25] P.F. Hoffman, D.P. Hawkins, C.E. Isachsen, S.A. Bowring, Precise U–Pb zircon ages for Early Damaran magmatism in the Summas Mountains and Welwitschia Inlier, northern Damara belt, Namibia, *Commun. Geol. Surv. Namibia* 11 (1996) 47–52.
- [26] P.F. Hoffman, A.J. Kaufman, G.P. Halverson, D.P. Schrag, A Neoproterozoic snowball Earth, *Science* 281 (1998) 1342–1346.
- [27] B. Huang, B. Xu, C. Zhang, Y. Li, R. Zhu, Paleomagnetism of the Baiysi volcanic rocks (ca. 740 Ma) of Tarim, Northwest China: A continental fragment of Neoproterozoic Western Australia? *Precambrian Res.* 142 (2005) 83–92.
- [28] W.T. Hyde, T.J. Crowley, S.K. Baum, W.R. Peltier, Neoproterozoic ‘Snowball Earth’ simulations with a coupled climate/ice sheet model, *Nature* 405 (2005) 425–430.
- [29] T.R. Ireland, T. Flöttmann, C.M. Fanning, G.M. Gibson, W.V. Preiss, Development of the Early Paleozoic Pacific margin of Gondwana from detrital zircon ages across the Delamerian orogen, *Geology* 26 (1998) 243–246.
- [30] R.M. Key, A.K. Liyungu, F.M. Njamue, V. Somwe, J. Banda, P.N. Mosley, R.A. Armstrong, The western arm of the Lufi lian Arc in NW Zambia and its potential for copper mineralization, *J. Afr. Earth Sci.* 33 (2001) 503–528.
- [31] B. Kilner, C. MacNiocaill, M. Brasier, Low-latitude glaciation in the Neoproterozoic of Oman, *Geology* 33 (2005) 413–416.
- [32] J.L. Kirschvink, Late Proterozoic low-latitude global glaciation: The Snowball Earth, in: J.W. Schopf, C. Klein (Eds.), *The Proterozoic Biosphere: A Multidisciplinary Study*, Cambridge University Press, 1992, pp. 51–52.
- [33] Z.X. Li, Mid- to low-latitude glaciation in Australia during Rodinia break-up: New paleomagnetic results from the ‘cap dolomite’ of the Walsh Tillite in southern Kimberley, *Precambrian Res.* 100 (2000) 359–370.
- [34] K. Lund, J.N. Aleinikoff, K.V. Evans, C.M. Fanning, SHRIMP U–Pb geochronology of Neoproterozoic Windermere Supergroup, central Idaho: implications for rifting of western Laurentia and synchronicity of Sturtian glacial deposits, *Geol. Soc. Am. Bull.* 115 (2003) 349–372.
- [35] M. Macouin, J. Besse, M. Ader, S. Gilder, Z. Yang, Z. Sun, P. Agrinier, Combined paleomagnetic and isotopic data from Doushantuo carbonates, South China: implications for the “snowball Earth” hypothesis, *Earth Planet. Sci. Lett.* 224 (2004) 387–398.
- [36] J.G. Meert, R. Van der Voo, The Neoproterozoic (1000–540 Ma) glacial intervals: No more Snowball Earth?, *Earth Planet. Sci. Lett.* 123 (1994) 1–13.
- [37] J.G. Meert, T.H. Torsvik, The making and unmaking of a Supercontinent: Rodinia revisited, *Tectonophysics* 375 (2003) 261–288.
- [38] J.G. Meert, R. Van der Voo, T.W. Payne, Paleomagnetism of the Catoctin volcanic province: A new Vendian-Cambrian apparent polar wander path for North America, *J. Geophys. Res.* 99 (B3) (1994) 4625–4641.
- [39] J.G. Meert, R. Van der Voo, S. Ayub, Paleomagnetic investigation of the Neoproterozoic Gagwe lavas and Mbozi complex, Tanzania and the assembly of Gondwana, *Precambrian Res.* 74 (1995) 225–244.
- [40] P. Morel, Palaeomagnetism of a Pan-African diorite: A Late Precambrian pole for western Africa, *Geophys. J. R. Astron. Soc.* 65 (1981) 493–503.
- [41] G. Murthy, C. Gower, M. Tubrett, R. Pätzold, Paleomagnetism of Eocambrian Long Range dykes and Double Mer Formation from Labrador, Canada, *Can. J. Earth Sci.* 29 (1992) 1224–1234.
- [42] J.K. Park, Paleomagnetic evidence for low-latitude glaciation during deposition of the Neoproterozoic Rapitan Group, Mackenzie Mountains, N.W.T., Canada, *Can. J. Earth Sci.* 34 (1) (1997) 34–39.
- [43] M.M. Pimentel, R.A. Fuck, N.F. Botelho, Granites and the geodynamic history of the Neoproterozoic Brasília belt, Central Brazil: a review, *Lithos* 46 (1999) 383–463.
- [44] R.P.E. Poorter, Palaeomagnetism of the Rogaland Precambrian (South-western Norway), *Phys. Earth Planet. Inter.* 5 (1972) 167–176.
- [45] W.V. Preiss, The Adelaide geosyncline of South Australia and its significance in Neoproterozoic continental reconstruction, *Precambrian Res.* 100 (2000) 21–63.
- [46] G.W. Ross, M.E. Villeneuve, U–Pb geochronology of stranger stones in Neoproterozoic diamictites, Canadian Cordillera: Implications for provenance and ages of deposition, *Radioactive Age and Isotopic Studies, Report 10: Geological Survey of Canada Current Research, 1997-F*, 1997, pp. 141–155.
- [47] P.W. Schmidt, G.E. Williams, The Neoproterozoic climatic paradox: Equatorial paleolatitude for Marinoan glaciation near sea level in South Australia, *Earth Planet. Sci. Lett.* 134 (1995) 107–124.
- [48] L.E. Sohl, N. Christie-Blick, D.V. Kent, Paleomagnetic polarity reversals in Marinoan (ca 600 Ma) glacial deposits of Australia: Implications for the duration of low-latitude glaciation in Neoproterozoic time, *Geol. Soc. Am. Bull.* 111 (1999) 1120–1139.
- [49] D.T.A. Symons, A.D. Chiasson, Paleomagnetism of the Callander Complex and the Cambrian apparent polar wander path for North America, *Can. J. Earth Sci.* 28 (1991) 355–363.
- [50] F.T. Tanczyk, P. Lapointe, W.A. Morris, P.W. Schmidt, A paleomagnetic study of the layered mafic intrusion at Sept-Iles, Quebec, *Can. J. Earth Sci.* 24 (1987) 1431–1438.
- [51] M.D. Thompson, S.A. Bowring, Age of the Squantum ‘tillite’, Boston basin, Massachusetts: U–Pb zircon constraints on terminal Neoproterozoic glaciation, *Am. J. Sci.* 300 (2000) 630–655 & 377–386.
- [52] T.H. Torsvik, K.C. Lohman, B.A. Sturt, Vendian glaciations and their relation to the dispersal of Rodinia: Paleomagnetic constraints, *Geology* 23 (1995) 727–730.
- [53] T.H. Torsvik, L.M. Carter, L.D. Ashwal, S.K. Bhushan, M.K. Pandit, B. Jamtveit, Rodinia refined or obscured: palaeomagnetism of the Malani igneous suite (NW India), *Precambrian Res.* 108 (2001) 319–333.
- [54] R.I.F. Trindade, E. Font, M.S. D’Agrella-Filho, A.C.R. Nogueira, C. Riccomini, Low-latitude and multiple geomagnetic reversals in the Neoproterozoic Puga cap carbonate, Amazon craton, *Terra Nova* 15 (2003) 441–446.
- [55] N.J. Turner, L.P. Black, M. Kamperman, Dating of Neoproterozoic and Cambrian Orogenies in Tasmania, *Austr. J. Earth Sci.* 45 (1998) 789–806.
- [56] D.A. Valencio, A.M. Sinito, J.F. Vilas, Paleomagnetism of Upper Precambrian rocks of the La Tinta Formation, Argentina, *Geophys. J. R. Astron. Soc.* 62 (1980) 563–575.
- [57] R. Van der Voo, The reliability of paleomagnetic data, *Tectonophysics* 184 (1990) 1–9.
- [58] M.T.D. Wingate, J.W. Giddings, Age and palaeomagnetism of the Mundine Well dyke swarm, Western Australia: implications

- for an Australia-Laurentia connection at 755 Ma, Precambrian Res. 100 (2000) 335–357.
- [59] B. Xu, P. Jian, H.F. Zheng, H.B. Zou, L.F. Zhang, D.Y. Liu, U-Pb zircon geochronology and geochemistry of Neoproterozoic volcanic rocks in the Tarim block of Northwest China: implications for the break-up of Rodinia supercontinent and Neoproterozoic glaciations, Precambrian Res. 136 (2005) 107–123.
- [60] S. Zhang, G. Jiang, J. Zhang, B. Song, M. Kennedy, N. Christie-Blick, U-Pb sensitive high-resolution ion microprobe ages from the Doushantuo Formation in south China: Constraints on Late Neoproterozoic glaciations, Geology 33 (2005) 473–476.
- [61] C. Zhou, R. Tucker, S. Xiao, Z. Peng, X. Yuan, Z. Chen, New constraints on the ages of Neoproterozoic glaciations in South China, Geology 32 (2004) 437–440.